



An All-Optical Trap for a Gram-Scale Mirror

Thomas Corbitt,¹ Yanbei Chen,² Edith Innerhofer,¹ Helge Müller-Ebhardt,³ David Ottaway,¹ Henning Rehbein,³
Daniel Sigg,⁴ Stanley Whitcomb,⁵ Christopher Wipf,¹ and Nergis Mavalvala¹

¹*LIGO Laboratory, Massachusetts Institute of Technology, Cambridge, Massachusetts 02139, USA*

²*Max-Planck-Institut für Gravitationsphysik, Am Mühlenberg 1, 14476 Potsdam, Germany*

³*Max-Planck-Institut für Gravitationsphysik (Albert Einstein Institute), Callinstraße 38, 30167 Hannover, Germany*

⁴*LIGO Hanford Observatory, Route 10, Mile marker 2, Hanford, Washington 99352, USA*

⁵*LIGO Laboratory, California Institute of Technology, Pasadena, California 91125, USA*

(Received 23 January 2007; published 13 April 2007)

We report on a stable optical trap suitable for a macroscopic mirror, wherein the dynamics of the mirror are fully dominated by radiation pressure. The technique employs two frequency-offset laser fields to simultaneously create a stiff optical restoring force and a viscous optical damping force. We show how these forces may be used to optically trap a free mass without introducing thermal noise, and we demonstrate the technique experimentally with a 1 g mirror. The observed optical spring has an inferred Young's modulus of 1.2 TPa, 20% stiffer than diamond. The trap is intrinsically cold and reaches an effective temperature of 0.8 K, limited by technical noise in our apparatus.

DOI: [10.1103/PhysRevLett.98.150802](https://doi.org/10.1103/PhysRevLett.98.150802)

PACS numbers: 07.10.Cm, 04.80.Nn

The change in dynamics caused by radiation pressure effects has been explored in many mechanical systems; its proposed applications include cooling toward the ground state of nanoelectromechanical systems (NEMS) or microelectromechanical systems (MEMS) [1–6], enhancing the sensitivity of gravitational wave (GW) detectors [7,8], and generation of ponderomotively squeezed light [9]. Two types of radiation pressure effects are evident in these systems: the optical restoring and viscous damping forces, both of which are generated by detuned optical cavities. Detuning a cavity to higher frequencies (blue detuning) gives rise to a restoring force, known as an optical spring [10–12], as well as an antidamping force due to the delay in the cavity response time. Conversely, detuning to lower frequencies (red detuning) gives rise to optical damping [13] along with an antirestoring force.

In NEMS and MEMS, optical (anti)restoring forces are typically negligible in comparison to the stiff mechanical suspension. However, optical damping produces cooling in a red-detuned cavity, while antidamping heats, or even leads to instability in a blue-detuned cavity [1–5,14,15]. In GW detectors, on the other hand, the optical spring force may dominate, since the mechanical suspension of their mirrors is very soft. The typical use of the optical spring effect in these systems is to enhance the sensitivity of the detector around the optical spring resonance. To achieve a restoring force, the cavity must be blue detuned, and the coincident optical antidamping force can both destabilize the cavity and give rise to parametric instabilities of the internal modes of its mirrors [7,16,17]. In general, whenever the radiation pressure of a single optical field dominates both the mechanical damping and restoring forces, the system is unstable due to the presence of a strong antidamping or antirestoring optical force.

Hence, until now this regime has been achieved only with the help of active feedback control to stabilize the dynamics [7,16].

Here we propose and demonstrate a technique that circumvents the optomechanical instability by using the radiation pressure of a second optical field, thus creating a stable optical trap for a 1 g mirror. This opens a new route to mitigating parametric instabilities in GW detectors and probing for quantum effects in macroscopic objects.

The experiment shown schematically in Fig. 1 was performed to demonstrate the optical trapping scheme. The 250 g input mirror of the $L = 0.9$ m long cavity is suspended as a pendulum with oscillation frequency of 1 Hz for the longitudinal mode. The 1 g end mirror is suspended by two optical fibers 300 μm in diameter, giving a natural frequency $\Omega_m = 2\pi \times 172$ Hz for its mechanical mode, with quality factor $Q_m = 3200$. On resonance, the intracavity power is enhanced relative to the incoming power by a resonant gain factor $4/\mathcal{T}_i \approx 5 \times 10^3$, where \mathcal{T}_i is the transmission of the input mirror, and the resonant linewidth (HWHM) is $\gamma = \mathcal{T}_i c/4L \approx 2\pi \times 11$ kHz.

If the resonance condition is exactly satisfied, the intracavity power depends quadratically on small changes in the length of the cavity. In this case the radiation pressure is only a second-order effect for the dynamics of the cavity. The constant (dc) radiation pressure is balanced through external forces; consequently, only fluctuations of the radiation pressure are considered here. If the cavity is detuned from the resonance condition, the intracavity power, and therefore the radiation pressure exerted on the mirrors, becomes linearly dependent on the length of the cavity, analogous to a spring. The resulting spring constant is given in the frequency domain by [11,16]

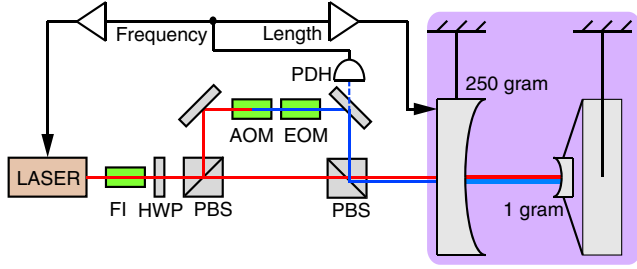


FIG. 1 (color online). Simplified schematic of the experiment. About 3 W of $\lambda_0 = 1064$ nm Nd:YAG laser light passes through a Faraday isolator (FI) before it is split into two paths by a half wave plate (HWP) and polarizing beam splitter (PBS) combination that allows control of the laser power in each path. The carrier (C) field comprises most of the light incident on the suspended cavity. About 5% of the light is frequency shifted by one free spectral range (161.66 MHz) using an acousto-optic modulator (AOM), and phase modulated by an electro-optic modulator (EOM); this subcarrier (SC) field can further be detuned from resonance to create a second optical spring. The two beams are recombined on a second PBS before being injected into the cavity, which is mounted on a seismic isolation platform in a vacuum chamber (denoted by the shaded box). A Pound-Drever-Hall (PDH) error signal derived from the SC light reflected from the cavity is used to lock it, with feedback to both the cavity length as well as the laser frequency. By changing the frequency shift of the SC, the C can be shifted off resonance by arbitrarily large detunings. The low power SC beam (blue) passes through the EOM and AOM before being recombined with the high power C beam (red).

$$K(\Omega) = K_0 \frac{[1 + (\delta/\gamma)^2 - (\Omega/\gamma)^2]}{[1 + (\delta/\gamma)^2 - (\Omega/\gamma)^2]^2 + 4(\Omega/\gamma)^2} \quad (1)$$

$$K_0 = \frac{2}{c} \frac{dP}{dL} = \frac{128\pi I_0 (\delta/\gamma)}{T_i^2 c \lambda_0} \left[\frac{1}{1 + (\delta/\gamma)^2} \right],$$

where Ω is the frequency of the motion, and δ and I_0 are the detuning and input power of the laser, respectively. Note the dependence of K_0 on the sign of δ . For $\delta > 0$ (in our convention), $K > 0$ corresponds to a restoring force, while $\delta < 0$ gives an antirestoring force; we do not explore this regime experimentally since it is always unstable for our system (see Fig. 2). The light in the cavity (for $\delta \ll \gamma$) responds to mirror motion on a time scale given by γ^{-1} . This delay has two effects. First, for high frequency motion ($\Omega \gtrsim \gamma$), the response of the cavity, and the corresponding radiation pressure, are reduced, and we see from Eq. (2) that $K(\Omega \gg \gamma) \approx K_0(\Omega/\gamma)^{-2}$. Second, the response of the cavity lags the motion, leading to an additional force proportional to the velocity of the mirror motion—a viscous force with damping coefficient given by [11,16]

$$\Gamma(\Omega) \equiv \frac{2K(\Omega)}{M\gamma[1 + (\delta/\gamma)^2 - (\Omega/\gamma)^2]}, \quad (2)$$

where M is the reduced mass of the two mirrors. Because

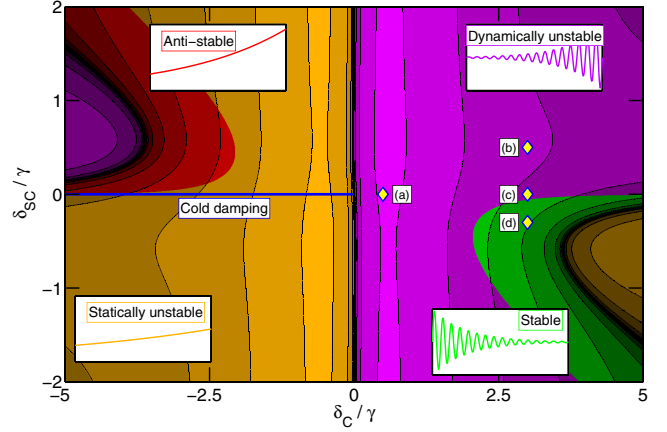


FIG. 2 (color online). Graphical representation of the total optical rigidity due to both optical fields, as a function of C and SC detuning, for fixed input power (power in the SC field is $\sim 1/20$ the C power) and observation frequency ($\Omega = 2\pi \times 1$ kHz). The shaded regions correspond to detunings where the total spring constant K and damping constant Γ are differently positive or negative. Specifically, “stable” corresponds to $K > 0$, $\Gamma < 0$, “antistable” to $K < 0$, $\Gamma > 0$, “statically unstable” to $K < 0$, $\Gamma < 0$, and “dynamically unstable” to $K > 0$, $\Gamma > 0$. The blue line denotes “cold damping” corresponding to $\delta_C < 0$ and $\delta_{SC} = 0$; i.e., the SC provides no optical force. The (logarithmically spaced) contours shown are scaled according to K : brighter regions have larger K . The labels (a)–(d) refer to the measurements shown in Fig. 3.

the cavity response lags the motion of the mirrors, a restoring spring constant implies a negative damping. Again we see that when both optical forces dominate their mechanical counterparts, the system must be unstable.

To stabilize the system we use two optical fields that respond on different time scales. One field should respond quickly, so that it makes a strong restoring force and only a weak antidamping force. The other field should respond slowly, so that it creates a strong damping force, with only a minor antirestoring force. This could be achieved with two cavities of differing bandwidths that share a common end mirror. However, it is simpler to use a single cavity and two fields with vastly different detunings. From Eqs. (1) and (2), taking $\Omega \ll \gamma$ (valid at the optical spring resonant frequency), we find

$$\frac{\Gamma}{K} = \frac{2/(M\gamma)}{1 + (\delta/\gamma)^2}; \quad (3)$$

we see that an optical field with larger detuning has less damping per stiffness. The physical mechanism for this is that at larger detunings the optical field resonates less strongly than for smaller detunings, so the time scale for the cavity response is shorter, leading to smaller optical damping. To create a stable system, we consider a carrier field (C) with large detuning $\delta_C \approx 3\gamma$ that creates a restoring force, but also a small antidamping force. To counteract the antidamping, a strong damping force is created

by injecting a subcarrier (SC) with small detuning $\delta_{SC} \approx -0.5\gamma$. For properly chosen power levels in each field, the resulting system is stable; we found a factor of 20 higher power in the carrier to be suitable in this case. To illustrate the behavior of the system at all detunings, the various stability regions are shown in Fig. 2 for this fixed power ratio. Point (d), in particular, shows that the system is stable for our chosen parameters.

Next we highlight some notable features of this optical trapping technique that were demonstrated experimentally using the apparatus of Fig. 1.

Extreme rigidity.—With no SC detuning and $\delta_C \approx 0.5\gamma$, the 172 Hz mechanical resonance of the 1 g mirror oscillator was shifted as high as 5 kHz [curve (a) in Fig. 3], corresponding to an optical rigidity of $K = 2 \times 10^6$ N/m. To put this number into perspective, consider replacing the optical mode with a rigid beam with Young's modulus E . The effective Young's modulus of this mode with area A of the beam spot (1.5 mm²) and length $L = 0.9$ m of the cavity, is given by $E = KL/A = 1.2$ TPa, stiffer than any known material (but also with very small breaking strength). Such rigidity is required to operate the cavity without external control; ambient motion would otherwise disrupt the cavity resonance condition.

Stabilization.—Also shown in Fig. 3 are curves corresponding to various C and SC detunings. In curves (b), (c), and (d), we detune the carrier by more than the cavity linewidth since the optical spring is less unstable for large δ_C . With no SC detuning, the optomechanical resonant frequency reaches $\Omega_{\text{eff}} = 2\pi \times 2178$ Hz, shown in

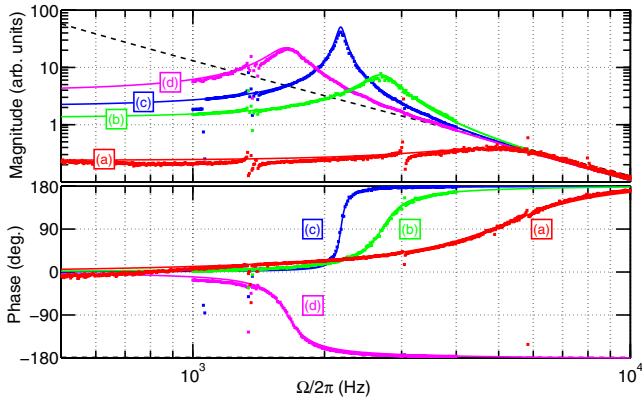


FIG. 3 (color online). The optical spring response for various power levels and detunings of the carrier and subcarrier. Measured transfer functions of displacement per force are shown as points, while the solid lines are theoretical curves. The dashed line shows the response of the system with no optical spring. An unstable optical spring resonance with varying damping and resonant frequency is produced when (a) $\delta_C = 0.5\gamma$, $\delta_{SC} = 0$; (b) $\delta_C = 3\gamma$, $\delta_{SC} = 0.5\gamma$; (c) $\delta_C = 3\gamma$, $\delta_{SC} = 0$; and it is stabilized in (d) $\delta_C = 3\gamma$, $\delta_{SC} = -0.3\gamma$. Note that the damping of the optical spring increases greatly as the optomechanical resonance frequency increases, approaching $\Gamma_{\text{eff}} \approx \Omega_{\text{eff}}$ for the highest frequency optical spring.

curve (c). Note that the optical spring is unstable, as evidenced by the phase increase of 180° about the resonance (corresponding to antidamping). Next we detune the subcarrier in the same direction as the carrier, shown in curve (b), which increases the resonant frequency and also increases the antidamping, demonstrated by the broadening of the resonant peak. For these two cases, electronic servo control is used to keep the cavity locked. If the control system is disabled, the amplitude of the cavity field and mirror oscillations grow exponentially. Remarkably, when the subcarrier is detuned in the opposite direction from the carrier, the optical spring resonance becomes stable, shown in curve (d), allowing operation of the cavity without electronic feedback at frequencies above 30 Hz; we note the change in phase behavior and the reduction of the resonant frequency. This shows how the frequency and damping of the optical spring can be independently controlled in the strong coupling regime.

Optical cooling.—The thermal excitation spectrum of the mirror, given by $S_F = 4k_B T \Gamma_m / M$, is not changed by the optical forces. It is informative to express this in terms of the optomechanical parameters Γ_{eff} , Ω_{eff} , and an effective temperature T_{eff} , such that the form of the equation is maintained. The effective temperature thus is given by

$$T_{\text{eff}} = T \frac{\Gamma_m}{\Gamma_{\text{eff}}} = T \frac{\Omega_m}{\Omega_{\text{eff}}} \frac{Q_{\text{eff}}}{Q_m}, \quad (4)$$

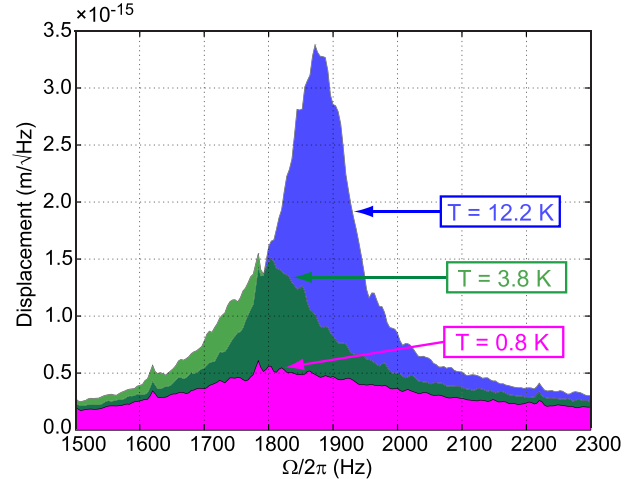


FIG. 4 (color online). The measured noise spectral density of the cavity length is shown for several configurations corresponding to different detunings. The lowest amplitude (magenta) curve corresponds to $\delta_C \approx 3$ and $\delta_{SC} \approx -0.5$. The other (green and blue) curves are obtained by reducing δ_{SC} and increasing δ_C in order to keep Ω_{eff} approximately constant, while varying Γ_{eff} . The spectrum is integrated between 1500 and 2300 Hz to calculate the rms motion of the oscillator mode, giving effective temperatures of 0.8, 3.8, and 12.2 K. The limiting noise source here is not thermal noise, but, in fact, frequency noise of the laser, suggesting that with reduced frequency noise even lower temperatures could be attained.

where $Q_i = \Omega_i/\Gamma_i$ ($i = m, \text{eff}$) is the quality factor of the oscillator. In the standard cold damping technique lower T_{eff} is achieved by decreasing Q_{eff} via the viscous radiation pressure damping. The optical spring effect results in further cooling by increasing the resonant frequency. The combination of both effects allows for much colder temperatures to be attained than with cold damping alone. This is relevant to experiments hoping to observe quantum effects in macroscopic objects, since it greatly reduces the thermal occupation number

$$N = \frac{k_B T_{\text{eff}}}{\hbar \Omega_{\text{eff}}}, \quad (5)$$

both by decreasing the effective temperature and increasing the resonant frequency.

In the current experiment the displacement spectrum is dominated by laser frequency noise at Ω_{eff} . We can nonetheless estimate the effective temperature of the optomechanical mode by measuring the displacement of the mirror, and equating $\frac{1}{2} K x_{\text{rms}}^2 = \frac{1}{2} k_B T_{\text{eff}}$, where x_{rms} is the rms motion of the mirror. To determine x_{rms} in our experiment, we measure the noise spectral density of the error signal from the cavity, calibrated by injecting a frequency modulation of known amplitude at 12 kHz. The displacement noise measured in this way is shown in Fig. 4. The lowest measured temperature of 0.8 K corresponds to a reduction in N by a factor of 2.5×10^3 .

In conclusion, we have exhibited a scheme that uses both the optical spring effect and optical damping from two laser fields to create a stable optomechanical system in which the dynamics are determined by radiation pressure alone. We experimentally demonstrated that the system is indeed stable, confirmed by deactivating the electronic control system and permitting the cavity to evolve freely at the dynamically relevant frequencies. We believe this is a useful technique for manipulating the dynamics of radiation pressure dominated systems, to quell their instabilities and examine their quantum behavior free from external control.

We would like to thank our colleagues at the LIGO Laboratory and the MQM group. We thank Steve Girvin, Mike Boyle, and Kentaro Somiya for helpful discussions in the preparation of this work. We gratefully acknowledge support from National Science Foundation Grants No. PHY-0107417 and No. PHY-0457264. Y.C.'s research

was supported by the Alexander von Humboldt Foundation (funded by the German Federal Ministry of Education and Research).

-
- [1] C.H. Metzger and K. Karrai, *Nature (London)* **432**, 1002 (2004).
 - [2] A. Naik, O. Buu, M.D. LaHaye, A.D. Armour, A.A. Clerk, M.P. Blencowe, and K.C. Schwab, *Nature (London)* **443**, 193 (2006).
 - [3] S. Gigan, H. Böhm, M. Paternostro, F. Blaser, G. Langer, J. Hertzberg, K. Schwab, D. Bäuerle, M. Aspelmeyer, and A. Zeilinger, *Nature (London)* **444**, 67 (2006).
 - [4] D. Kleckner and D. Bouwmeester, *Nature (London)* **444**, 75 (2006).
 - [5] O. Arcizet, P.-F. Cohadon, T. Briant, M. Pinard, and A. Heidmann, *Nature (London)* **444**, 71 (2006).
 - [6] A. Schliesser, P. Del'Haye, N. Nooshi, K.J. Vahala, and T.J. Kippenberg, *Phys. Rev. Lett.* **97**, 243905 (2006).
 - [7] O. Miyakawa, R. Ward, R. Adhikari, M. Evans, B. Abbott, R. Bork, D. Busby, J. Heefner, A. Ivanov, M. Smith, R. Taylor, S. Vass, A. Weinstein, M. Varvella, S. Kawamura, F. Kawazoe, S. Sakata, and C. Mow-Lowry, *Phys. Rev. D* **74**, 022001 (2006).
 - [8] A. Buonanno and Y. Chen, *Phys. Rev. D* **65**, 042001 (2002).
 - [9] T. Corbitt, Y. Chen, F. Khalili, D. Ottaway, S. Vyatchanin, S. Whitcomb, and N. Mavalvala, *Phys. Rev. A* **73**, 023801 (2006).
 - [10] A. Buonanno and Y. Chen, *Phys. Rev. D* **65**, 042001 (2002).
 - [11] V.B. Braginsky and S.P. Vyatchanin, *Phys. Lett. A* **293**, 228 (2002).
 - [12] B.S. Sheard, M.B. Gray, C.M. Mow-Lowry, D.E. McClelland, and S.E. Whitcomb, *Phys. Rev. A* **69**, 051801 (2004).
 - [13] S. Mancini, D. Vitali, and P. Tombesi, *Phys. Rev. Lett.* **80**, 688 (1998).
 - [14] D. Kleckner, W. Marshall, M. de Dood, K. Dinyari, B.-J. Pors, W. Irvine, and D. Bouwmeester, *Phys. Rev. Lett.* **96**, 173901 (2006).
 - [15] P.F. Cohadon, A. Heidmann, and M. Pinard, *Phys. Rev. Lett.* **83**, 3174 (1999).
 - [16] T. Corbitt, D. Ottaway, E. Innerhofer, J. Pelc, and N. Mavalvala, *Phys. Rev. A* **74**, 021802 (2006).
 - [17] T.J. Kippenberg, H. Rokhsari, T. Carmon, A. Scherer, and K.J. Vahala, *Phys. Rev. Lett.* **95**, 033901 (2005).